

Bias dependence of magnetoresistance in Fe–Al₂O₃ granular thin films

M. A. S. Boff, J. Geshev, and J. E. Schmidt

Instituto de Física—UFRGS, C.P. 15051, 91501-970, Porto Alegre, RS, Brazil

W. H. Flores

Laboratório Nacional de Luz Síncrotron, C.P. 6192, 13083-970, Campinas, SP, Brazil

A. B. Antunes, M. A. Gusmão, and S. R. Teixeira

Instituto de Física—UFRGS, C.P. 15051, 91501-970, Porto Alegre, RS, Brazil

(Received 26 November 2001; accepted for publication 26 March 2002)

This paper reports on the magnetotransport behavior of Fe–Al₂O₃ granular thin films when the injected dc current is varied. The electric resistance as a function of temperature, magnetoresistance, and the current vs applied bias potential measurements were used to characterize the samples. It was found that the transport mechanism which best describes the electronic properties of these samples is variable range hopping. Non-Ohmic behavior was observed and is claimed as responsible for the great modification of the electronic characteristics of the system as a function of the applied bias potential. Inversion of the tunneling magnetoresistance is observed for applied bias potential greater than 3 V. Such inverted magnetoresistance comes from the activation of low resistivity tunneling paths that are promoted by increasing the bias potential. An expression is proposed to describe the magnetoresistance behavior. © 2002 American Institute of Physics. [DOI: 10.1063/1.1479481]

I. INTRODUCTION

Metal/insulator granular systems composed of grains of a ferromagnetic element (such as Fe, Co, or Ni) immersed in an insulating matrix have been extensively studied in the last few years, mainly because they can present unique magnetotransport properties that make them good candidates for future technological applications. Granular solids can be easily obtained either by sputtering or by melt spinning, and their microstructure can be significantly altered by thermal treatment methods prior or after its fabrication, thus allowing the production of a broad variety of granular structures, characterized by their particle size distribution and density. The electronic transport in these systems is believed to be determined by spin-dependent tunneling.^{1–7} Recently, several groups have shown that Fe–Al₂O₃ and Co–Al₂O₃ exhibit high values of tunneling magneto-resistance.^{8–11} This work reports on a detailed study of the electronic transport properties of the Fe–Al₂O₃ granular thin films, through the ensemble analysis of the measurements of current vs applied bias (I vs V), electric resistance vs temperature (R vs T), and magnetoresistance (MR). Here MR is defined as $MR = 100 \times [R(0) - R(H)]/R(0)$, where H is the applied magnetic field.

II. EXPERIMENT

The Fe–Al₂O₃ films were obtained by coevaporation of Fe and Al₂O₃ at room temperature, in a system with a base pressure better than 1×10^{-8} mbar, using as substrates pre-oxidized Si wafers. Both thickness and deposition rates, the variation of which allows different compositions to be obtained, have been monitored by a computer controlled quartz balance. Rutherford backscattering spectrometry, using 1.5 MeV α particles, confirmed that our set of 1000 Å thick

samples had an average metal volume fraction x of 0.27, 0.33, 0.41, and 0.48 respectively. Room temperature X-ray diffractometry employing Cu $K\alpha$ radiation showed only broad peaks with $\Delta 2\theta = 2.6^\circ$ corresponding to (110) reflections of bcc Fe grains. No substantial differences were observed between the spectra even when the linewidth of the (110) reflection of iron was monitored. The samples appear to be textured in a (110) direction. No reflections corresponding to the Al₂O₃ were observed. Using the Scherrer formulas, we concluded that the samples are composed of bcc Fe clusters of 43 Å average size, embedded in an amorphous Al₂O₃ matrix. In addition, considering the samples as homogeneous, the distance between two neighbor grains around 40 Å (overestimated), and that the distance between the electrodes is 1 mm for an applied potential of 20 V, the maximum ΔV between two nearest individual grains was estimated to be less than 0.2 mV, which is smaller than $k_B T$ (k_B is the Boltzmann constant). This means that, even for an applied potential of 20 V, the low field regime probably holds.³

Plots of I versus V and of R versus T for temperatures ranging from 4.2 to 300 K, were obtained using a four-point method, applying a constant dc current and monitoring the change of V in a current-in-plane geometry. The resistance was obtained using $R = V/I$. The MR was measured using a dc injected current ranging from 1 μ A to 20 mA.

III. RESULTS AND DISCUSSION

Figure 1 shows the R versus T curve for the sample with $x = 0.41$, where a negative temperature coefficient is observed. For low bias potential, as in the case of Fig. 1, all samples show R versus T curves, typical of granular systems, i.e., R increases when the temperature decreases.^{1–3} One can notice that there is a temperature T_0 below which R

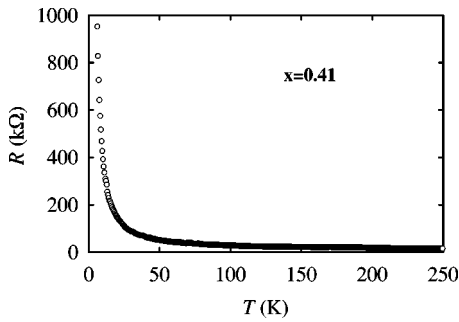


FIG. 1. R vs T curve for the sample with $x=0.41$.

risers very rapidly. This temperature is an intrinsic property of the sample, and its physical interpretation depends on the theory used to explain it. T_0 will depend on the structural characteristics of the sample if the conductivity process is determined by thermal activation mechanisms, or it will depend on the localization length of the electrons if the electronic conductivity is governed by variable range hopping. Samples with larger metallic volume fraction show a less pronounced increase of R when T decreases than those with small metal volume fraction. This behavior can be described by the equation³

$$R = R_0 \exp(T_0/T)^\alpha, \tag{1}$$

where T_0 depends on the metallic concentration and α can assume values of 1/2 for thermally activated hopping, and 1/4 for variable range hopping.⁶ Figure 2 presents the $\ln R$ versus $T^{-1/4}$ plots as well as the fitting curves obtained by using Eq. (1). The T_0 values derived from these fitting curves are also given in this figure. For $\alpha=1/4$, T_0 is related to electronic localization length ξ through the relation $T_0 = \beta_M / (k_B \xi^3 g_0)$, where $\beta_M = 1.5$ and g_0 is the constant Mott density of states.¹² The $T^{-1/4}$ dependence for the $\ln R$ vs $T^{-1/4}$ curves given in Fig. 2 resulted in a better fitting than the $T^{-1/2}$ dependence for the whole temperature range, that is, from 300 to 4.2 K. The possible interpretation is that $T^{-1/4}$ dependence appears because the transport, in the present case, is between grains of larger sizes, where charge effects have low influence. In apparent opposition, recent

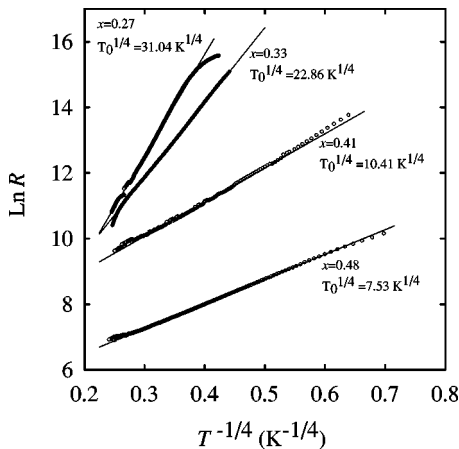


FIG. 2. $\ln R$ vs $T^{-1/4}$ plots for samples with $x=0.27, 0.33, 0.41,$ and 0.48 for low applied dc current. The solid lines are the fittings using Eq. (1).

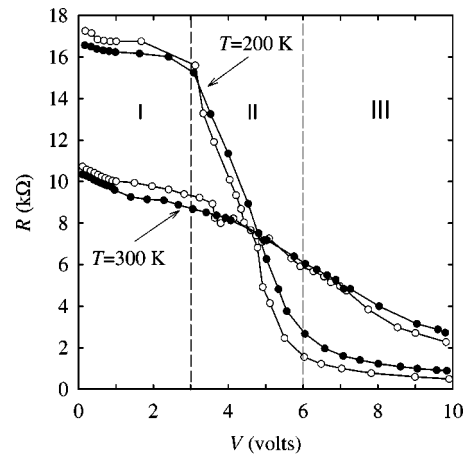


FIG. 3. R vs V curves at 200 and 300 K for the sample with $x=0.33$. The magnetic field is equal to 0 and 60 kOe, white and black dots, respectively.

report in a similar system states that a $T^{-1/2}$ dependence was found,¹³ within the temperature range of 300 to 100 K. It should be emphasized that the mean Fe grain size, in the present case, is greater than the one reported by Ge *et al.*¹³ So, we conclude that the electronic transport for these samples occurs via the variable range hopping.

The I versus V measurements were made at different temperatures for applied bias potential ranging from 0 to 20 V. All samples presented a non-Ohmic behavior. The trends of these curves are better viewed through the R versus V plots. Figure 3 presents the R versus V curves for the sample with $x=0.33$ at 200 and 300 K with applied magnetic field of 0 and 60 kOe, white and black dots, respectively. A non-Ohmic behavior is observed, and a well defined transition from high to low resistivity can be identified for applied bias greater than 3 V, this effect being more pronounced at low temperatures. Note that such non-Ohmic behavior is not expected for these systems. It is also important to note that the MR inverts when the applied bias increases. This effect can be clearly seen by comparing the curves with white and black dots. Associated to these observations one can distinguish three different regions in Fig. 3: region I, going from 0 to 3 V, where the tunneling can be described by variable range hopping, a transition region, called region II, where new paths start to be turned on, decreasing the resistance of the samples, and region III, above 6 V, where the low resistivity paths are blocked at low temperatures. The low resistivity paths can be activated by a long range hopping, e.g., tunneling between more distant grains through channels that are turned on when the electric field is increased. For the samples with $x=0.33$ and 0.41 in region I, R increases when the temperature decreases but for high bias, region III, R decreases with the lowering of the temperature. This behavior is unexpected for granular systems. The values of the bias potential necessary to change the conductivity, as one goes from regions I to II and from regions II to III, depend on the volume fraction of metal and on the structural characteristics of the system. The transition in the conductivity presented in regions II is unexpected and unexplained by the existing theories.

Figure 4 shows the $\ln R$ dependence of the sample with

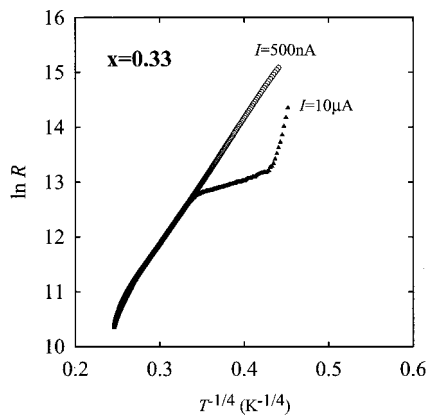


FIG. 4. $\ln R$ vs $T^{-1/4}$ for the sample with $x=0.33$ for two different applied dc currents.

$x=0.33$ on $T^{-1/4}$ for two different currents. The same non-Ohmic characteristics presented in the I versus V curves shown before are seen. When the injected dc current is high enough, a plateau appears in a certain temperature range. This plateau can be ascribed to the low resistivity paths that are turned on when the bias potential increases as in the R versus V curves. Note that the resistance is almost independent of the temperature. In the plateau region, where low resistivity paths are active, the parameter T_0 is very small due to the high value of the localization length of the electrons. When the temperature decreases, these low resistivity paths start to be blocked due to the Coulomb blockade effects. As the Coulomb blockade starts, the resistance increases back to the same values of the low bias case (Fig. 4).

Going back to Fig. 3 it can be seen that MR inverts when the bias potential increases. In region I, the resistance is lower for $H=60$ kOe as compared with the resistance for $H=0$ Oe, leading to a positive MR, while for high bias, region III, the situation is inverted, producing a negative MR. This effect can be clearly seen in Figs. 5 and 6 for the sample with $x=0.41$, where a plot of R vs H at 200 and 40 K are presented. The magnetoresistance of this sample was measured with an injected dc current ranging from 1 μ A (region I) to 20 mA (region II, near region III) as indicated in Figs. 5 and 6. The magnetoresistance at low bias potential (or low dc current) shows only spin dependent tunneling. For high bias (or high dc current) two components of MR are evidenced. One is ascribed to an inversion of the electron spin polarization, as described previously by Sharma¹⁴ and De Tereza,¹⁵ as due to spin dependent tunneling, in the low magnetic field region. The other component is independent of the magnetization and does not saturate up to $H=30$ kOe. For the variable range hopping conductivity process, this component is associated to the decrease of the transmission probability when the magnetic field increases.

This effect can be explained using the wave-function shrinkage model.¹⁶ For high bias potential, the resistance of the sample decreases due to the activation of low resistivity paths, as depicted in Fig. 3, in regions II and III. In this case, the conductivity is mainly due to d electrons.¹⁷ If the distance of hopping between two grains is sufficiently large, the ΔV between these grains also increases. If this value is high

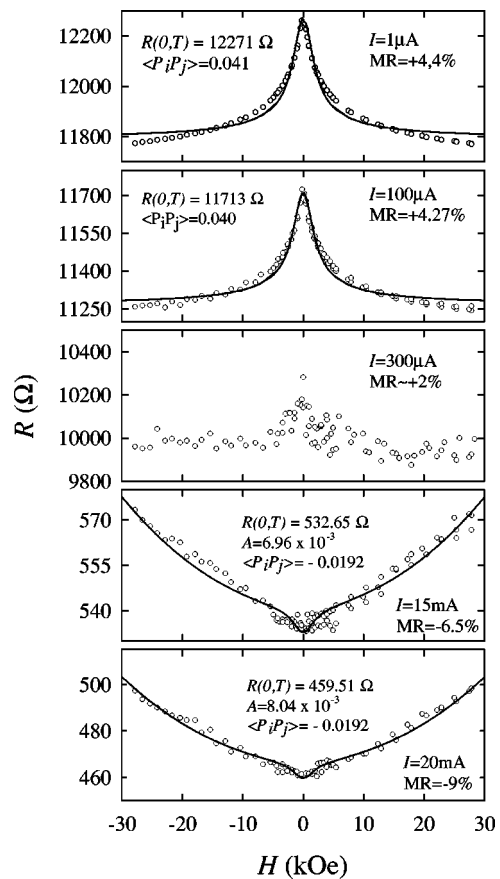


FIG. 5. Magnetoresistance of the sample with $x=0.41$ at 200 K for different dc currents, where the parameters are indicated in the figure. The solid lines are the fittings using Eq. (2).

enough, the difference between the Fermi level of the d band of the two grains will be high and could give rise to a spin inversion. This can be understood as follows: let us consider the d bands of two Fe grains separated by a certain amount, as displayed in Fig. 7. Here we use bulk d bands only for illustration; the real d bands for small grains should be different. In this figure we also consider that the magnetic moments of each grain are aligned parallel to each other. At low bias, the hopping takes place between grains short distance apart, corresponding to small ΔV , lowering by a small amount the Fermi level of the grain at the right-hand side, Fig. 7(a). As demonstrated in the figure, there are more empty states in the spin up than in the spin down d bands (see the shaded area in the figure) so the tunneling current will be composed by spin up electrons mainly, generating the expected positive magnetoresistance. However, when the bias increases, the probability of long distance hopping also increases. If the hopping takes place through long distances, ΔV between the two grains will be large enough, so it is expected that the Fermi level of the grain at the right-hand side will move down to a position as depicted by Fig. 7(b). In this case, the number of empty states at the spin down band is greater than those at the spin up d bands (see the shaded area in the figure), thus the electronic current will be composed mainly by spin down electrons. The polarization of the tunneling current should be considered as the mean polarization of all possible paths for the tunneling electrons,

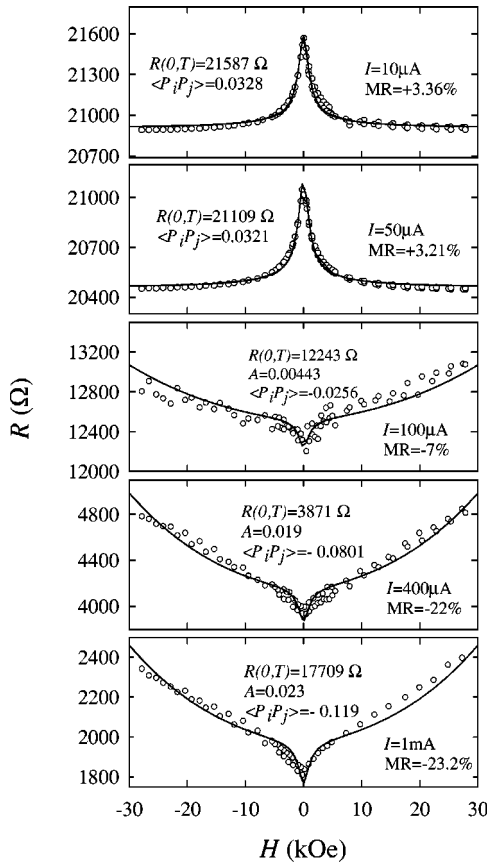


FIG. 6. Magnetoresistance of the sample with $x=0.41$ at 40 K for different dc currents, where the parameters are indicated in the figure. The solid lines are the fittings using Eq. (2).

which can also assume negative values as illustrated by Fig. 7(b). In the general case, we consider $\langle P_i P_j \rangle$ as the average value of all tunneling trajectories among all grains that participate in the tunneling processes. To take into account the two components that appear in the R versus H curves, we rewrite the expression for the resistance¹⁰ as follows:

$$R(H, T) = \frac{R(0, T)}{1 + \langle P_i P_j \rangle m^2} \exp(AH^2), \quad (2)$$

where the normalized magnetization m of a superparamagnetic system is given by the Langevin function, i.e., $m = \coth(\mu H/k_B T) - k_B T/\mu H$. Here, μ 's are the magnetic moments of the grains, $R(0, T) = R$, as in Eq. (1), is the electric resistance of the sample when the applied magnetic field is equal to 0, $A = t_1 (e^2 \xi^4 / \hbar^2) (T_0 / T)^{3/4}$, the parameter t_1 is predicted to be ≈ 0.00248 , and T_0 is the characteristic temperature for the case when $\alpha = 1/4$ in Eq. (1). The exponential term that appears in Eq. (2), takes into account the component on the magnetoresistance that is independent on the magnetization.^{16,18} When A is very small, this exponential term goes to unity and the resistance is only dependent on the magnetization and on the mean polarization of the electronic current. The mean value $\langle P_i P_j \rangle$ is due to the spin polarization of the electronic current, that is not the same for all grains that contribute to the tunneling conduction, but depends on the hopping distance and the potential difference between the grains. For very close grains and/or low poten-

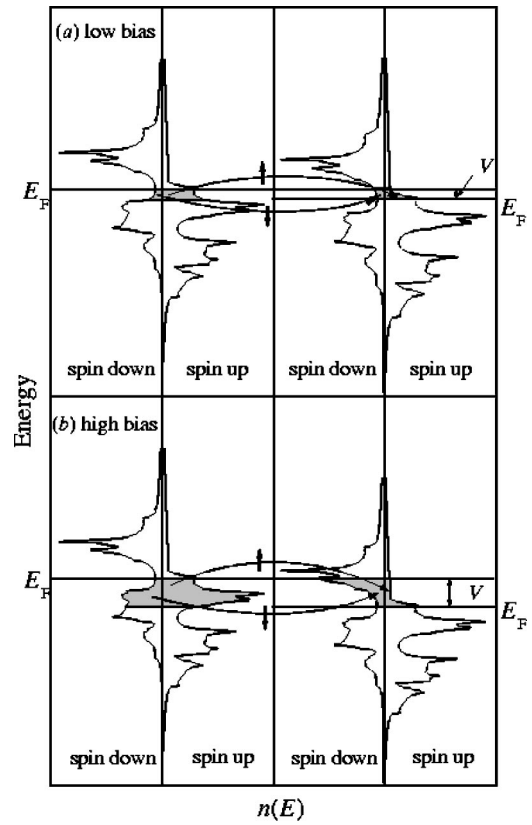


FIG. 7. Density of states for two Fe grains separated by a certain distance. Bulk Fe data are used in order to illustrate the spin inversion mechanism. (a) Low bias and short distance hopping; (b) high bias, long distance hopping.

tial difference between them, $P_i = P_j$ and $\langle P_i P_j \rangle \approx P^2$; however, if the two grains are distant enough, the potential difference can be high and $\langle P_i P_j \rangle$ can be very different from P^2 , even assuming negative values as depicted in Fig. 7(b). If $\langle P_i P_j \rangle$ is negative, high values of magnetoresistance can be achieved, as shown in Figs. 5 and 6. For nonmagnetic samples $m=0$, and the resistance will depend only on the magnetic field value.

Using Eq. (2) with dc current values of 1 μA , 100 μA , 15 mA, and 20 mA at 200 K, and assuming that all grains have the same magnetic moment value, namely $\mu = 4000 \mu_B$, the fittings of the magnetoresistance curves are presented as solid lines in Fig. 5. Taking the magnetic moment of 2.22 μ_B per Fe atom and 2.87 \AA for the lattice constant of bcc Fe, it can be demonstrated that the moment of 4000 μ_B corresponds to a mean grain size of approximately 43 \AA . This is actually the room temperature value extracted from the x-ray measurements. For lower temperature, $T=40$ K, the magnetoresistance curves for dc currents of 10 μA , 50 μA , 100 μA , 400 μA , and 1 mA were fitted through Eq. (2) (see Fig. 6), using a magnetic moment of 1600 μ_B , which corresponds to a mean grain size of approximately 32 \AA . The association of these smaller particles to the behavior of the magnetoresistance at low temperatures has also been observed by Honda *et al.*¹⁹ for Fe-(SiO₂) granular films. As can be seen, the fitting curves are in very good agreement with the experimental results. It is possible to explain the MR component, which is independent of the

magnetization through the increase of the localization length ξ that is only the nonconstant term of the parameter A . For low applied dc current, region I in Fig. 2, ξ is very short, the exponential term approaches unity and $P_i = P_j = P^2$, thus Eq. (2) reduces to the same equation presented by Zhu and Wang.¹⁰

The two grain sizes, used in the superparamagnetic fit of the experimental data cited above, can be compared with the critical diameter for superparamagnetic behavior, D_{sp} (for particles of sizes smaller than D_{sp} , thermal fluctuations will enable spontaneous magnetization reversal to occur; the larger particles have their moments blocked in their original direction until a sufficiently large reversal field is applied). The thermal activation effects are usually examined via calculations of the relaxation time τ for the reversal of the magnetization direction, given by the Arrhenius type equation²⁰

$$\tau^{-1} = f_0 \exp(-\Delta E/k_B T). \quad (3)$$

Here f_0 is the attempt frequency whose value is generally accepted to be 10^9 s^{-1} ; recent measurements, however, have shown that this value can be as high as 10^{12} for iron oxide materials²¹ or even 10^{13} for Fe-(SiO₂) granular films.²² ΔE is the height of the anisotropy energy barrier prohibiting rotation, where $\Delta E = K_u V_p$ for uniaxial anisotropy particles and $\Delta E = K_c V_p/4$ for cubic anisotropy particles with positive first order anisotropy constant K_c , which is the case of bcc iron. K_u is the uniaxial anisotropy constant and V_p is the particle volume.

It is not difficult to calculate the maximum value for D_{sp} for a given temperature. Considering spherical particles with cubic magnetocrystalline anisotropy, assuming a measurement time of 100 s and also assuming the largest value for f_0 , i.e., $f_0 = 10^{13} \text{ s}^{-1}$, one obtains $D_{sp}^{\max} \approx 6.4 (k_B T/K_c)^{1/3}$. Using the temperature variation of K_c for bulk iron,²³ D_{sp}^{\max} is estimated to be 137 and 242 Å for $T = 40$ and 200 K, respectively. Moreover, if the uniaxial (shape) anisotropy predominates over the cubic one, and assuming $f_0 = 10^9 \text{ s}^{-1}$, one can estimate the lowest value for D_{sp} as $D_{sp}^{\min} \approx 3.6 (k_B T/K_u)^{1/3}$. If $K_u = 0.67 K_c$, which is the lowest K_u value above which the uniaxial anisotropy dominates over the cubic one for a disordered system with random elongation directions,²⁴ the corresponding D_{sp}^{\min} values are 88 and 155 Å for $T = 40$ and 200 K, respectively. As can be seen, all these values are rather larger than the ones used in the fittings performed here, thus assuring that the latter are representatives of superparamagnetic particles at the temperatures under consideration.

For high applied dc current, regions II and III in Fig. 2, ξ increases and consequently A also. The exponential term raise up with the magnetic field, and as a consequence, the electric resistance increases and does not saturate, which is different from the spin dependent term. For applied dc currents equal to 15 and 20 mA at 200 K, $\langle P_i P_j \rangle$ is negative, thus MR is inverted. The behavior of the magnetoresistance indicates that the transition in the I versus V dependence can be related to the activation of some low resistivity tunneling paths that appear for a certain bias potential, namely 3 V. This leads to an increase of ξ itself which promotes an enhancement of the tunneling probability of electrons with a

decrease of the total resistance. On the other hand, for high H values, the increase of ξ will enhance the interference effects in the electronic wave functions that leads to a raise in the sample resistance with the applied magnetic field. As shown in Figs. 5 and 6, this component of the magnetoresistance does not saturate even for fields as high as 30 kOe.

IV. CONCLUSIONS

It was found that the basic electronic transport mechanism in our samples is associated to a variable range hopping. The I versus V measurements showed a non-Ohmic behavior caused by a change from a high to a low resistivity electronic regime that occurs when the localization length ξ increases with the bias potential, as expected when low resistivity channels are turned on. Three regions, which are dependent on the bias potential, temperature, and volume fraction of the metal, could be identified in the R versus V curves (Fig. 3). These three regions were characterized as follows: region I, with small ξ , where the conductivity is due to hopping between near neighboring grains. In this region, the samples present high resistivity. The electric resistance decreases when a magnetic field is applied and a spin dependent tunnel magnetoresistance is observed (positive MR). This region is very well described by the usual theories.^{3,9} In region II, for bias potential greater than 3 V, new paths with low resistivity associated to long localization length of electrons are created, and the total resistance of the sample decreases. In this region, an inversion of the MR is observed. The existing theories for granular systems^{3,4} cannot explain the electronic transport in this region. Region III occurs for high bias potential, where the resistance of the samples decreases and then saturates. In this region, high values of inverted MR can be achieved. The inverted MR has two components, one is due to an inversion of the spin polarization of tunneling electrons, and the other one is associated to the interference effects on the electron wave functions that increase the resistance of the sample when the magnetic field increases. This effect is well described by the wave-function shrinkage model.^{16,18}

The low resistivity of region III is related to an increase of the localization length of the electrons that occurs when the bias potential is increased. Dependence of MR on applied bias potential was observed. The MR inverts from positive to negative when the applied bias increases above a certain value that depends on the volume fraction of the iron. A modified expression for the resistance was proposed in order to explain the dependence of the MR on the applied bias potential.

ACKNOWLEDGMENTS

This work has been partly supported by the Brazilian financial agencies Conselho Nacional de Desenvolvimento Científico e Tecnológico (CNPq), Coordenação de Aperfeiçoamento de Pessoal de Nível Superior (CAPES), Financiadora de Estudos e Projetos (FINEP), and Fundação de Amparo à Pesquisa do Estado do Rio Grande do Sul (FAPERGS).

- ¹J. Simmons, *J. Appl. Phys.* **34**, 1793 (1963).
- ²S. Sankar, B. Dieny, and A. E. Berkowitz, *J. Appl. Phys.* **81**, 5512 (1997).
- ³B. Abeles, *Applied Solid State Science: Advances in Materials and Device Research*, edited by R. Wolfe (Academic, New York, 1976), p. 1.
- ⁴K. M. Unruh and C. L. Chien, *Nanomaterials: Synthesis, Properties, and Applications*, edited by A. S. Edelstein and R. C. Camarata (Institute of Physics, Bristol, 1996), Chap. 14.
- ⁵B. Abeles, P. Sheng, M. D. Coutts, and Y. Arie, *Adv. Phys.* **24**, 407 (1975).
- ⁶P. Sheng, B. Abeles, and Y. Arie, *Phys. Rev. Lett.* **31**, 44 (1973).
- ⁷N. A. Gershenfeld, J. E. VanCleve, W. W. Webb, H. E. Fischer, N. A. Fortune, J. S. Brooks, and M. J. Graf, *J. Appl. Phys.* **64**, 4760 (1988).
- ⁸S. H. Ge, S. B. Zhang, J. H. Chi, Z. G. Zhang, C. X. Li, and R. J. Gan, *J. Phys. D* **33**, 917 (2000).
- ⁹S. Mitani, S. Takahashi, K. Takanashi, K. Yakushiji, S. Maekawa, and H. Fujimori, *Phys. Rev. Lett.* **81**, 2799 (1998).
- ¹⁰T. Zhu and Y. J. Wang, *Phys. Rev. B* **60**, 11 918 (1999).
- ¹¹Y. H. Huang, J. H. Hsu, and J. W. Chen, *IEEE Trans. Magn.* **33**, 3556 (1997).
- ¹²R. Rosenbaum, N. V. Lien, M. R. Graham, and M. Witcomb, *J. Phys.: Condens. Matter* **9**, 6247 (1997).
- ¹³S. H. Ge, S. B. Zhang, J. H. Chi, Z. G. Zhang, C. X. Li, and R. J. Gan, *J. Phys. D* **33**, 917 (2000).
- ¹⁴M. Sharma, S. X. Wang, and J. H. Nickel, *Phys. Rev. Lett.* **82**, 616 (1999).
- ¹⁵J. M. De Tereza, A. Barthélémy, A. Fert, J. P. Comtour, R. Lyonnet, F. Montaigne, P. Seneo, and A. Vaurès, *Phys. Rev. Lett.* **82**, 4288 (1999).
- ¹⁶R. Rosenbaum, T. Murphy, E. Palm, S. Hannahs, and B. Brant, *Phys. Rev. B* **63**, 094426 (2001).
- ¹⁷G. G. Cabrera and N. Garcia, The Los Alamos archive, code number cond-mat/0106123.
- ¹⁸B. I. Shklovskii and B. Z. Spivak, *Hopping Transport in Solids*, edited by M. Pollak and B. Shklovskii, *Modern Problems in Condensed Matter Sciences Vol. 28* (Elsevier Science, Amsterdam, 1991), Chap. 9.
- ¹⁹S. Honda, T. Okada, M. Nawate, and M. Tokumoto, *Phys. Rev. B* **56**, 14 566 (1997).
- ²⁰L. Néel, *Ann. Geophys.* **5**, 99 (1949).
- ²¹D. P. E. Dickson, N. M. K. Reid, C. Hunt, H. D. Williams, M. El-Hilo, and K. O'Grady, *J. Magn. Magn. Mater.* **125**, 345 (1993).
- ²²G. Xiao, S. H. Liou, A. Levy, J. N. Taylor, and C. L. Chien, *Phys. Rev. B* **34**, 7573 (1986).
- ²³R. M. Bozorth, *J. Appl. Phys.* **8**, 575 (1937).
- ²⁴J. Geshev, A. D. C. Viegas, and J. E. Schmidt, *J. Appl. Phys.* **84**, 1488 (1998).